2008 American Control Conference
Westin Seattle Hotel, Seattle, Washington, USA
June 11-13, 2008

An Anti-Windup Technique for LMI Regions with Applications to a Fluid Power System

Brandon Hencey, *Member, IEEE*, and Andrew Alleyne, *Senior Member, IEEE*

Abstract—**The anti-windup problem seeks to minimize the closed loop performance deterioration due to input nonlinearities, such as saturation, for a given linear time-invariant plant and controller. This paper presents a linear matrix inequality (LMI) based method that attempts to minimize performance deterioration while explicitly restricting the anti-windup closed loop dynamics. The restriction placed on the dynamics is described via LMI regions, which is a form of regional pole placement. Finally, the techniques discussed in this paper are demonstrated on an electro-hydraulic testbed.**

Index Terms—**Windup, Control nonlinearities, Robust stability, Linear matrix inequality regions**

I. INTRODUCTION

Given an unconstrained closed loop system composed of a linear time invariant (LTI) plant and stabilizing controller, the objective of the anti-windup problem, as defined in [7], is to mitigate the adverse effects of input nonlinearities, such as saturation. As shown in Figure 1, an anti-windup compensator Λ augments the controller in the presences of the input nonlinearity. The anti-windup compensator is optimized with respect to some performance metric. The induced ℓ_2 and $\mathcal{L}_2$ norms from disturbance w to regulated output z are two commonly used performance metrics for continuous and discrete time [4], [5], [7], [9].

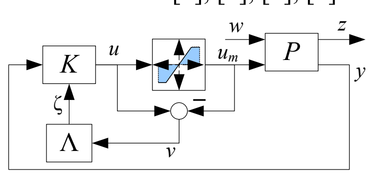

Figure 1: General closed loop system with anti-windup

Linear matrix inequality (LMI) regions, a class of convex regions in the complex plane, are used to describe $\mathcal{D}$-stability, a modified notion of stability [2],[6]. In particular, [2] discusses quadratic $\mathcal{D}$-stability with respect to the H_∞ norm over an LMI region, and presents LMI conditions that recover the continuous and discrete-time as special cases. This paper extends the concept of quadratic $\mathcal{D}$-stability to the anti-windup problem, thereby allowing specifications for the anti-windup closed loop dynamics to be defined using intuitive complex plane constraints. The static anti-windup compensator case was initially investigated in [5], whereas this work focuses upon the dynamic, as well as static, anti-windup compensator synthesis conditions ensuring quadratic $\mathcal{D}$-stability.

The problem is defined in terms of quadratic $\mathcal{D}$-stability using LMI regions in Section II. Section III.A develops LMI conditions to evaluate the performance of an anti-windup closed loop system. In Section III.B, anti-windup compensator synthesis conditions arise from a linearizing change of variables applied to the conditions of Section III.A. The conditions for continuous-time and discrete-time static [7], [9] and plant-order dynamic [4] anti-windup syntheses are included as special cases of the anti-windup synthesis conditions presented. In Section IV, an electro-hydraulic powertrain test bed detailed in [10] is used as a practical example to demonstrate how the anti-windup compensator design technique may be used to restrict the anti-windup closed loop dynamics for digital prototyping.

II. BACKGROUND AND PROBLEM DEFINITION

A. Notation

For a matrix A, A^* denotes its complex conjugate transpose. $\mathbb{H}^n$ is the set of n by n Hermitian matrices. The matrix inequality $A > B$ means that $A, B \in \mathbb{H}^n$ and $A - B$ is positive definite. ImA is the image subspace of the linear mapping represented by the matrix A. Let the matrix with its block diagonal described by $M_1,\ldots,M_N$ and zero elsewhere be denoted as $\operatorname{diag}(M_1,\ldots,M_N)$.

B. Quadratic $\mathcal{D}$-Stability

In order to discuss robust pole placement, let us introduce some notation for LMI regions, as defined in the [2].

Definition 1: An LMI region is a subset of the complex plane that is defined as

$$\mathcal{D} \triangleq \{s \in \mathbb{C} : f_{\mathcal{D}}(s) < 0\}$$

where

$$f_{\mathcal{D}}(s) = L + Ms + M^* s^*, \; L, M \in \mathbb{R}^{q \times q}. \tag{1}$$

The open left half plane (OLHP) and open unit disc correspond to $f_{\mathcal{D}}(s) = s^* + s$ and $f_{\mathcal{D}}(s) = ss^* - 1$, respectively. Note that $f_{\mathcal{D}}(s) = ss^* - 1$ is placed in the form (1) via the Schur complement [1],[6].

This work was supported in part by the Center for Compact and Efficient Fluid Power, grant number Army W911NF-04-1-0067, and Caterpillar, Inc.

B. Hencey and A. Alleyne are with Dept. of Mechanical and Industrial Engineering, University of Illinois Urbana-Champaign, 1206 W. Green St., Urbana, IL 61801, (email: hencey@uiuc.edu and alleyne@uiuc.edu).

978-1-4244-2079-7/08/$25.00 ©2008 AACC.

Definition 2: If every eigenvalue of the matrix $A \in \mathbb{R}^{n\times n}$ lies in the LMI region $\mathcal{D}$, then A is considered to be $\mathcal{D}$-stable . •

Definition 3: The linear time-varying uncertain system

$$\delta[x(t)] = A(\Delta(t))x(t)\,, \tag{2}$$

where δ signifies a linear time operator such as the derivative for the continuous-time case and the forward step for discrete-time, is *quadratic $\mathcal{D}$-stable* if there exists $X \in \mathbb{H}^n$ such that

$$M_{\mathcal{D}}(X, A(\Delta(t))) < 0 \text{ and } X > 0$$

for every $\Delta(t)$ in the uncertainty set $\mathcal{S}_{\Delta(t)}$. •

For the remainder of this paper, state variables x, uncertainties Δ, and other consequent variables are implicitly a function of t, unless otherwise noted. Consider the linear time-varying uncertain system described by the linear time-invariant (LTI) system

$$\begin{cases} \delta[x] = Ax + Bw \\ z = Cx + Dw \end{cases}, \tag{3}$$

interconnected with $w(t) = \Delta(t)z(t)$, where $\Delta(t) \in \mathrm{S}_\Delta$ and

$$\mathrm{S}_\Delta \triangleq \{\Delta(t) : z^*[I \quad \Delta^*]\Theta[I \quad \Delta^*]^* z \geq 0\,, \forall z(t) \in \mathbb{R}^{n_z}\}\,, \tag{4}$$

for an appropriately partitioned Θ. Define M_1 and M_2 as the factorization for a given $M = M_1 M_2 \in \mathbb{R}^{q\times q}$ where $M_1, M_2^* \in \mathbb{R}^{q\times r}$ and r=rank(M), and define the matrices $U \in \mathbb{R}^{s\times n_z}$ and $\Sigma \in \mathbb{R}^{s\times s}$ as satisfying $\Theta_{11} = U^*\Sigma^{-1}U$, where s=rank(Θ_{11}). The reader is directed to [6, Theorem 1] for the proof of *Lemma 1* and the discussion of equivalence to bounded and positive real lemmas for discrete-time and continuous time.

Lemma 1 - Quadratic $\mathcal{D}$-Stability for Uncertain System: Suppose the system (2) is described by the interconnection of (3) and $w(t) \triangleq \Delta(t)z(t)$, with $\Delta(t) \in \mathrm{S}_\Delta$ in (4). Then the linear system is quadratically $\mathcal{D}$-stable and well-defined if there exists positive definite $X \in \mathbb{H}^n$ such that

$$\begin{bmatrix} \Omega_{xx} & \Omega_{xw} & \Omega_{zx}^* \\ \Omega_{xw}^* & \Omega_{ww} & \Omega_{zw}^* \\ \Omega_{zx} & \Omega_{zw} & \Omega_{zz} \end{bmatrix} < 0\,,$$

where $\Omega_{xx} = M_{\mathcal{D}}(X, A)$, $\Omega_{zx} = M_2 \otimes UC$,

$$\Omega_{zw} = I_r \otimes UD \qquad \Omega_{ww} = I_r \otimes (D\Theta_{21} + \Theta_{21}^* D^* + \Theta_{22})$$

$$\Omega_{zz} = -I_r \otimes \Sigma \qquad \Omega_{xw} = M_1 \otimes XB + M_2^* \otimes C^*\Theta_{21}^*.$$

C. Class of Input Nonlinearities

Rather than solving the anti-windup problem for a particular decentralized input nonlinearity, $u_m = \phi(t,u)$, we consider a class of time-varying input nonlinearities

$$\phi \in \mathcal{S}_\Phi \triangleq \{\phi(t,u) : \phi^*(t,u)(u - \phi(t,u)) \geq 0, \forall (t,u)\}\,,$$

which corresponds with the sector [0,1] of the circle criterion. Also, sufficient information is assumed to be known about the time-varying input nonlinearity such that an online measurement or estimate of u_m is available. The class of time-varying nonlinearities includes the saturation function, the dead-zone nonlinearity, and control switching, but the saturation function is the prevalent input nonlinearity of practical interest here. Let the decentralized saturation function be defined as

$$\mathrm{sat}(u) = [\mathrm{sat}_1(u_1)^*, \ldots, \mathrm{sat}_{n_u}(u_{n_u})^*]^*\,.$$

The departure from the *unconstrained closed loop system* $(u_m = u)$, the closed loop system void of input-nonlinearities, is described by

$$v(t) = \psi(t,u) \triangleq u - \phi(t,u)\,, \tag{5}$$

where $\psi \in \mathcal{S}_\Phi$ if and only if $\phi \in \mathcal{S}_\Phi$.

D. Problem Definition

The unconstrained closed loop system is described by the interconnection of the $\mathcal{D}$-Stable LTI plant

$$P \triangleq \begin{cases} \delta x_p = A_p x_p + B_{p,w} w + B_{p,u} u_m \\ z = C_{p,z} x_p + D_{p,zw} w + D_{p,zu} u_m \\ y = C_{p,y} x_p + D_{p,yw} w + D_{p,yu} u_m \end{cases}, \tag{6}$$

and stabilizing LTI controller

$$K \triangleq \begin{cases} \delta x_k = A_k x_k + B_{k,y} y + \zeta_1 \\ u = C_{k,u} x_k + D_{k,uy} y + \zeta_2 \end{cases}, \tag{7}$$

where $x_p \in \mathbb{R}^{n_p}$, $x_k \in \mathbb{R}^{n_k}$, $w \in \mathbb{R}^{n_w}$, $u_m \in \mathbb{R}^{n_u}$, $z \in \mathbb{R}^{n_z}$, $y \in \mathbb{R}^{n_y}$, and $[\zeta_1^*, \zeta_2^*] = 0$. Note that an important part of the anti-windup design paradigm is that K has been designed without consideration for the input-nonlinearities.

As represented by the relation $u_m(t) = u(t) - v(t)$ in Figure 1, $v(t) \neq 0$ may be viewed as a disturbance, produced by the input nonlinearity $\psi(t,u)$, acting on the unconstrained closed loop system. Driven by $v(t)$, the linear anti-windup compensator mitigates the negative impact upon the closed loop performance via $\zeta(t)$. Let the unconstrained closed loop system driven by $v(t)$ and $\zeta(t)$ be written as

$$H \triangleq \begin{cases} \delta x_{cl} = A_{cl} x_{cl} + B_{cl,v} v + B_{cl,w} w + B_{cl,\zeta} \zeta \\ u = C_{cl,u} x_{cl} + D_{cl,uv} v + D_{cl,uw} w + D_{cl,u\zeta} \zeta \\ z = C_{cl,z} x_{cl} + D_{cl,zv} v + D_{cl,zw} w + D_{cl,z\zeta} \zeta \end{cases}, \tag{8}$$

where $x_{cl} = [x_p^*, x_k^*]^*$ and the matrices in (8) are defined explicitly by (6), (7), and $u_m(t) = u(t) - v(t)$. The unconstrained closed loop system is augmented with a linear anti-windup compensator

$$\Lambda \triangleq \begin{cases} \delta x_\lambda = A_\lambda x_\lambda + B_\lambda v \\ \zeta = C_\lambda x_\lambda + D_\lambda v \end{cases}, \tag{9}$$

where $x_\lambda \in \mathbb{R}^{n_\lambda}$, and $\zeta = [\zeta_1^* \quad \zeta_2^*]^*$, that minimizes the performance deterioration due to the input-nonlinearity.

For the following definition, we use a definition of performance similar in nature to [4, Definition 3].

Definition 4: The linear anti-windup compensator Λ guarantees a *quadratic performance level* γ if the uncertain anti-windup closed loop system (8), (9), $v(t)=\psi(t,u)$, $w=\Delta(t)z$ satisfies:

(a) the interconnection is well defined for all $\psi\in\mathcal{S}_\Phi$ and $\Delta\in\mathcal{S}_\Delta(\gamma)$, where

$$\mathcal{S}_\Delta(\gamma)\triangleq\{\Delta(t): z^*z-\gamma^2(\Delta z)^*(\Delta z)\geq 0, \forall(t,z)\}, \quad (10)$$

(b) the anti-windup closed loop system is quadratic $\mathcal{D}$-Stable. •

III. ANTI-WINDUP ANALYSIS AND SYNTHESIS

Section III.A presents LMI conditions for establishing a quadratic performance level γ for an anti-windup closed loop system. In seeking to optimize quadratic performance level in Section III.B, synthesis conditions for Λ arise from a linearizing change of variables applied to conditions presented in Section III.A.

A. Anti-windup Performance Analysis

For the analysis of the anti-windup closed loop system, assume the plant P in (6), controller K in (7), and anti-windup compensator Λ in (9) are given, whereas the input uncertainty $\phi\in\mathcal{S}_\Phi$ and $\Delta\in\mathcal{S}_\Delta(\gamma)$ are not. Let the LTI portion of the anti-windup closed loop system be defined as

$$G\triangleq\begin{cases}\delta x=Ax+B_v v+B_w w\\ u=C_u x+D_{uv}v+D_{uw}w,\\ z=C_z x+D_{zv}v+D_{zw}w\end{cases} \quad (11)$$

where $x=[x_p^*,x_k^*,x_\lambda^*]^*$ and the matrices A, B_v, B_w, C_u, C_z, D_{uv}, D_{uw}, D_{zv}, and D_{zw} are determined by the interconnections of the systems given in (8) and (9).

Theorem 1: Given G in (11), $f_\mathcal{D}(s)$ in (1), and $\gamma>0$, the anti-windup closed loop system guarantees quadratic performance level of γ if there exists a symmetric matrix $X>0$, and a diagonal matrix $W>0$ such that

$$\begin{bmatrix}\Omega_{xx} & \Omega_{xv}+\Omega_{ux}^* & \Omega_{xw} & \Omega_{zx}^*\\ \Omega_{xv}^*+\Omega_{ux} & \Omega_{uv}+\Omega_{uv}^* & \Omega_{uw} & \Omega_{zv}^*\\ \Omega_{xw}^* & \Omega_{uw}^* & -\gamma I & \Omega_{zw}^T\\ \Omega_{zx} & \Omega_{zv} & \Omega_{zw} & -\gamma I\end{bmatrix}<0, \quad (12)$$

where, $\Omega_{xx}=M_\mathcal{D}(X,A)$,

$$\begin{bmatrix}\Omega_{xv} & \Omega_{xw}\end{bmatrix}=\begin{bmatrix}M_1\otimes XB_v & M_1\otimes XB_w\end{bmatrix}$$

$$\begin{bmatrix}\Omega_{ux}^* & \Omega_{zx}^*\end{bmatrix}=\begin{bmatrix}M_2^*\otimes C_u^*W & M_2^*\otimes C_z^*\end{bmatrix}$$

$$\begin{bmatrix}\Omega_{uv} & \Omega_{uw}\\ \Omega_{zv} & \Omega_{zw}\end{bmatrix}=\begin{bmatrix}I_r\otimes W(D_{uv}-I) & I_r\otimes WD_{uw}\\ I_r\otimes D_{zv} & I_r\otimes D_{zw}\end{bmatrix}.$$

Proof: For a given trajectory $u(t)$, define $\Psi(t)$ satisfying $\Psi(t)u=\psi(t,u)$. Thus at every point in time, $\bar{\Delta}=\text{diag}(\Psi,\Delta)$ satisfies $[I\ \ \bar{\Delta}^*]\Theta[I\ \ \bar{\Delta}^*]^*\leq 0$ for any diagonal matrix $W>0$, where

$$\Theta=\begin{bmatrix}\Theta_{11} & \Theta_{12}^*\\ \Theta_{12} & \Theta_{22}\end{bmatrix}=\begin{bmatrix}\text{diag}(0,I/\gamma) & \text{diag}(W,0)\\ \text{diag}(W,0) & \text{diag}(-2W,-I\gamma)\end{bmatrix}. \quad (13)$$

Given G in (11) and Θ, *Lemma 1* yields the above sufficient conditions. □

Remark 1: Consider an LMI region that is the intersection of multiple LMI regions

$$\mathcal{D}=\bigcap_{i=1}^N\mathcal{D}_i, \quad (14)$$

described by $f_\mathcal{D}(s)=\text{diag}(f_{\mathcal{D}1}(s),\ldots,f_{\mathcal{D}N}(s))$. If *Theorem 1* verifies a quadratic performance level of γ for each $f_{\mathcal{D}i}(s)$ $i=1,\ldots,r$, then a quadratic performance level γ is satisfied for $\mathcal{D}$. •

Remark 2: The OLHP case of Theorem 1 concurs with the continuous-time results presented in Theorem 1 of [4]. •

B. Anti-windup Compensator Synthesis

Based on Theorem 1, simultaneously searching for X and an anti-windup compensator satisfying (12) is a bilinear matrix inequality. This section applies a linearizing change of variables to the conditions of Theorem 1 in order to construct conditions for the existence of an anti-windup.

Consider a positive definite symmetric matrix Y

$$Y=\begin{bmatrix}R & N\\ N^* & M\end{bmatrix}=\begin{bmatrix}S^{-1} & X_{12}\\ X_{12}^* & X_{22}\end{bmatrix}^{-1}=X^{-1}, \quad (15)$$

where $R,S\in\mathbb{H}^{n_{CL}}$, $M,X_{22}\in\mathbb{H}^{n_\lambda}$, $N,X_{12}\in\mathbb{R}^{n_{CL}\times n_\lambda}$, and $\text{rank}(R-S)=n_\lambda$. From (15), $R-S=NM^{-1}N^*$ and

$$Y\begin{bmatrix}0 & I_{n_{CL}}\\ M^{-1}N^* & -M^{-1}N^*\end{bmatrix}=\begin{bmatrix}R-S & S\\ N^T & 0\end{bmatrix}. \quad (16)$$

Post-multiplying (16) by $\text{diag}(V,I)$ produces $Y\Pi_2=\Pi_1$, where

$$\Pi_1=\begin{bmatrix}NM^{-1}N_1^* & S\\ N_1^* & 0\end{bmatrix},\ \Pi_2=\begin{bmatrix}0 & I_{n_{CL}}\\ M^{-1}N_1^* & -M^{-1}N^*\end{bmatrix},$$

$\Pi_2^*\Pi_1=\text{diag}(Q_{11},S)$, $V=[V_1,V_2]\in\mathbb{R}^{n_{cl}\times n_{cl}}$ is orthonormal, $V^*V=I$, $V_2\in\mathbb{R}^{n_{cl}\times n_\lambda}$ forms the basis for the null space of $(R-S)$, $N_1=V_1^*N\in\mathbb{R}^{n_\lambda\times n_\lambda}$, and $Q_{11}=N_1M^{-1}N_1^*\in\mathbb{H}^{n_\lambda}$ is positive definite.

Theorem 2: Given the plant P in (6), the unconstrained controller K in (7), $f_\mathcal{D}(s)$ in (1), an integer $n_\lambda\leq n_{cl}$, an orthonormal matrix $[V_1\ \ V_2]\in\mathbb{R}^{n_{cl}\times n_{cl}}$, $V_1\in\mathbb{R}^{n_{cl}\times n_\lambda}$, and $\gamma>0$; there exists a linear anti-windup compensator Λ of order n_λ such that the anti-windup closed loop system has a quadratic performance level γ if there exists $(\hat{A}_\lambda,\hat{B}_\lambda,\hat{C}_\lambda,\hat{D}_\lambda)$, $S\in\mathbb{H}^{n_{cl}}$, $Q_{11}\in\mathbb{H}^{n_\lambda}$, and diagonal $U\in\mathbb{R}^{n_u}$ satisfying

$$U>0, S>0, Q_{11}>0, \quad (17)$$

$$\Omega=\begin{bmatrix}\Omega_{xx}+\Omega_{xx}^* & \Omega_{xv}+\Omega_{ux}^* & \Omega_{xw} & \Omega_{zx}^*\\ \Omega_{xv}^*+\Omega_{ux} & \Omega_{uv}+\Omega_{uv}^* & \Omega_{uw} & \Omega_{zv}^*\\ \Omega_{xw}^* & \Omega_{uw}^* & -I\gamma & \Omega_{zw}^*\\ \Omega_{zx} & \Omega_{zv} & \Omega_{zw} & -I\gamma\end{bmatrix}<0, \quad (18)$$

where

$$\Omega_{xx} = \frac{L}{2} \otimes \begin{bmatrix} Q_{11} & 0 \\ 0 & S \end{bmatrix} + M \otimes \begin{bmatrix} \hat{A} & 0 \\ A_{cl}V_1Q_{11} - V_1\hat{A} + B_{cl,\zeta}\hat{C} & A_{cl}S \end{bmatrix}$$

$$\Omega_{ux} = M_2 \otimes \begin{bmatrix} C_{cl,u}V_1Q_{11} + D_{cl,u\zeta}\hat{C} & C_{cl,u}S \end{bmatrix}$$

$$\Omega_{zx} = M_2 \otimes \begin{bmatrix} C_{cl,z}V_1Q_{11} + D_{cl,z\zeta}\hat{C} & C_{cl,z}S \end{bmatrix}$$

$$\Omega_{xv} = M_1 \otimes \begin{bmatrix} \hat{B} \\ B_{cl,v}U + B_{cl,\zeta}\hat{D} - V_1\hat{B} \end{bmatrix}, \ \Omega_{xw} = M_1 \otimes \begin{bmatrix} 0 \\ B_{cl,w} \end{bmatrix}$$

$$\begin{bmatrix} \Omega_{uv} & \Omega_{uw} \\ \Omega_{zv} & \Omega_{zw} \end{bmatrix} = \begin{bmatrix} I_r \otimes (D_{cl,uv}U + D_{cl,u\zeta}\hat{D}_\lambda - U) & I_r \otimes D_{cl,uw} \\ I_r \otimes (D_{cl,zv}U + D_{cl,z\zeta}\hat{D}_\lambda) & I_r \otimes D_{cl,zw} \end{bmatrix}.$$

Proof: Start by assuming (17) and (18) are satisfied. Choose N_1, N, M satisfying $Q_{11} = N_1M^{-1}N_1^*$ and $V_1Q_{11}V_1^* = NM^{-1}N^*$. Noting Π_1^{-1} exists because N_1 and S are full rank, apply the congruence transformation

$$T = \text{diag}\left(I_q \otimes \Pi_1^{-1}, I_r \otimes W, I\right)$$

to (18) and set $W = U^{-1}$, $R = S + NM^{-1}N^*$

$$A_\lambda = MN_1^{-1}\hat{A}_\lambda N_1^{-*} \quad B_\lambda = MN_1^{-1}\hat{B}_\lambda W$$

$$C_\lambda = \hat{C}_\lambda N_1^{-*} \quad D_\lambda = \hat{D}_\lambda W.$$

in order to show (12) is satisfied for X in (15). □

The matrix V_1 describes the choice of subspace for $(R-S) = V_1Q_{11}V_1^*$ while satisfying the rank constraint $\text{rank}(R-S) = n_\lambda$. Choosing $V_1 = [I_{n_p}, 0_{n_p \times n_k}]^*$ produces what is known as a *plant-order anti-windup compensator* $(n_\lambda = n_p)$, whereas choosing $V_2 = I_{n_{cl}}$ produces what is known as a *static anti-windup compensator* $(n_\lambda = 0)$.

Remark 3: For the static anti-windup compensator synthesis, the conditions of *Theorem 2* are equivalent to Theorem 1 in [9] and Theorem 3 in [7] for the special cases $f_{\mathcal{D}}(s) = ss^* - 1$ and $f_{\mathcal{D}}(s) = s^* + s$, respectively. For more details on the static anti-windup synthesis for LMI regions see [5]. •

Remark 4: If M in $f_{\mathcal{D}}(s)$ has rank(M)=1, the Elimination Lemma [1] can be used to produce equivalent conditions from (18) that are devoid of $(\hat{A}_\lambda, \hat{B}_\lambda, \hat{C}_\lambda, \hat{D}_\lambda)$. For the plant-order anti-windup compensator, those equivalent conditions correspond to the necessary and sufficient conditions in [4,Proposition 2]. For $r = \text{rank}(M) > 1$, the simplicity offered by the Elimination Lemma breaks down due to the added complexity of the structured LMI variable

$$\Lambda = \begin{bmatrix} I_r \otimes A_\lambda & I_r \otimes B_\lambda \\ I_r \otimes C_\lambda & I_r \otimes D_\lambda \end{bmatrix}.$$

The authors of [8] further elaborate on the resulting difficulty of the necessary and sufficient conditions related to the Elimination Lemma for structured LMI variables. •

Corollary 1: Suppose $n_\lambda = n_p$ and $V_1 = [I_{n_p}, 0_{n_p \times n_k}]^*$. Then there exists $\gamma > 0$ such that (17) and (18) are feasible if A_p and A_{cl} in (6) and (8) are $\mathcal{D}$-stable .

Proof: Note that we may assume $D_{p,yu}$=0 without loss of generality. Let $\hat{A} = A_pQ_{11}$, $\hat{C}^* = -Q_{11}C_{p,y}^*[B_{k,y}^*, D_{k,uy}^*]$, $\hat{D} = 0$, and $\hat{B} = B_{p,u}U$. Since A_p and A_{cl} are $\mathcal{D}$-stable , there exists Q_{11} and S such that (17) and (18) are satisfied for sufficiently large γ. □

It may also be shown via *Corollary 1* that if Im[V_1] contains the subspace $\text{Im}[I_{n_p}, 0]^*$ and A_p and A_{cl} are $\mathcal{D}$-stable , then there exists a solution for some finite $\gamma > 0$ such that (17) and (18) are feasible.

Remark 5: As in Remark 1, a less conservative condition may be constructed for an LMI region that is the intersection of multiple LMI regions (14). *Theorem 2* can be evaluated for each $f_{\mathcal{D}_i}(s)$ by replacing S with S_i and searching for $(\hat{A}_\lambda, \hat{B}_\lambda, \hat{C}_\lambda, \hat{D}_\lambda)$, Q_{11}, S_i, and U that satisfy (17) and (18). Then the reconstruction of X_i and $(A_\lambda, B_\lambda, C_\lambda, D_\lambda)$ can be accomplished as outlined in the proof of *Theorem 2*. •

IV. PRACTICAL EXAMPLE

In this section, the Earthmoving Vehicle Powertrain Simulator (EVPS) at the University of Illinois at Urbana-Champaign is used as a testbed to demonstrate the utility of the quadratic $\mathcal{D}$-stability in anti-windup compensator design. Although the work presented in this paper also supports the discrete-time case, the following example was chosen as a novel approach to a problem often encountered when digitally prototyping continuous-time anti-windup compensators.

The continuous-time controller and linear anti-windup compensators are implemented on a hardware-in-the-loop system using a Runge-Kutta fixed-step solver and Wincon 3.2 software designed by Quanser Consulting Inc. As a general rule of thumb, the Nyquist frequency $\omega_s = \pi/T_s$ (T_s=0.002) should be several times faster than the fastest dynamics. As noted in Turner & Postlethwaite (2004), the continuous-time anti-windup compensator synthesis presented in [4] can yield excessively fast poles, which cause difficulties in the digital implementation of the anti-windup compensator.

The following presents an example where excessively fast anti-windup closed loop poles were generated via the algorithms discussed in [4]. Attempts at implementing the resulting anti-windup compensators proved unsuccessful. However, Theorem 2 was used to explicitly constrain the poles, thereby enabling the resulting anti-windup compensators to be successfully implemented.

A. Experiment Setup

The EVPS is a hardware-in-the-loop testbed capable of emulating earthmoving powertrains [10] and similar hydraulic equipment. In the following experiment, the EVPS was utilized to emulate a hydrostatic powertrain with a continuously variable transmission (CVT). The prime mover for the powertrain, shown in Figure 2, consists of a compression ignition engine emulated through a three-phase induction motor. The emulated engine drives the variable-displacement pump, i.e. the CVT in the powertrain, and the pressurized hydraulic fluid drives a hydraulic motor with a disturbance torque applied to its shaft.

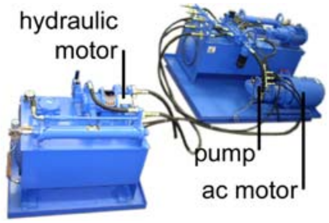

Figure 2: Hydrostatic powertrain schematic

The linearized model is a variance of the model structure presented in [10]. The engine speed n_e and hydraulic motor speed n_m, as well as the corresponding reference signals $n_{e,r}$ and $n_{m,r}$, are measurements available to the controller. The powertrain is controlled through the engine fuel index γ_e, and swash plate angle α. The reduced-order model linear model is:

$$P_{yu} = \begin{cases} \dot{x}_p = A_p x_p + B_{p,u} u \\ y = C_{p,y} x_p + D_{p,yu} u \end{cases}$$

where $u = [\gamma_e \quad \alpha]^*$, $x_p = [n_e \quad p \quad n_m]^*$,

$$A_p = \begin{bmatrix} -0.8409 & -9.699 & 0 \\ 0.1803 & 0.8461 & -0.5271 \\ -2.03 & 2440 & -28.01 \end{bmatrix},\; C_{p,y} = \begin{bmatrix} 1 & 0 & 0 \\ 0 & 0 & 1 \end{bmatrix},$$

$$B_{p,u} = \begin{bmatrix} 29.15 & -22.11 \\ 0.01547 & 6.976 \\ 0.02799 & -11.54 \end{bmatrix}, \text{ and } D_{p,yu} = \begin{bmatrix} 0 & 0 \\ 0 & 0 \end{bmatrix}.$$

B. Feedback Controller Design

The control objective is to simultaneously track a desired engine speed and motor speed. In order to fulfill robust performance requirements, the controller $\hat{K}$ was designed to minimize the H_∞ gain from w to z of the unconstrained $(u_m = u)$ closed loop system shown in Figure 3. The weighting matrices on the various signals in Figure 3 are as follows

$$W_r = \text{diag}(40,40),\; W_u = \text{diag}(0.30,0.15),$$

$$W_e = \text{diag}(0.0667,0.400), \text{ and}$$

$$W_n = \begin{cases} \dot{x}_{Wn} = -65.13 x_{Wn} - 3.256 n_e + 32.56 n_m \\ z_3 = -x_{Wn} - 0.05 n_e + 0.5 n_m \end{cases}.$$

The controller $\hat{K}$ was designed via the `hinfmix` algorithm available in the LMI Control Toolbox, [3]. For this example, the magnitude of the anti-windup closed loop poles will be limited to $\omega_{max}=\omega_s/4\approx 350$ rad/s. In order to allow some extra bandwidth for the anti-windup compensator design, the unconstrained closed loop LMI region was chosen as the OLHP intersected with a disk with a radius of 300 rad/s centered at the origin.

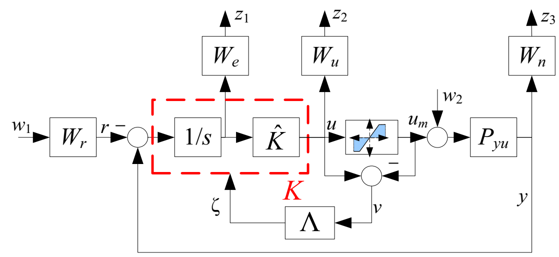

Figure 3: Anti-windup closed loop system

C. Anti-windup Compensator Design

The ability of the transmission to meet the command tracking objectives is limited by input constraints on the fuel index γ_e and swashplate angle α. The limited fuel index reflects a limited power range, whereas the limited swashplate angle reflects a limited gear ratio. When the inputs saturate, the integrators in Figure 3 continue to wind-up. In order to counter the wind-up problem, an anti-windup compensator is employed, as shown in Figure 3. The anti-windup compensator design is based upon the same H_∞ weightings as the controller design. In order to avoid the algebraic loops discussed in [4], [9], we restrict $\tilde{D}_\lambda^*$ to the form $\hat{D}_\lambda^* = [\hat{D}_{\lambda 1}^*, 0_{n_u \times n_u}]$, where $\hat{D}_{\lambda 1} \in \mathbb{R}^{n_k \times n_u}$.

First, we consider designing the anti-windup compensators for continuous-time using $f_{\mathcal{D}_1}(s) = s + s^*$. For the static anti-windup synthesis $(V_2 = I_{n_{cl}})$, Theorem 2 yields the anti-windup compensator

$$\Lambda_{s1} = \begin{bmatrix} -23.81 & -9.051 & -2.992 & 13.65 & 2.163 & 5.156 & 465.7 & 220.3 & 0 & 0 \\ 0.998 & -1.125 & 0.365 & 0.013 & 0.079 & -0.188 & -6.703 & 24.79 & 0 & 0 \end{bmatrix}^*$$

Similarly, denote the plant order $(V_1 = [I_n, 0]^*)$ anti-windup compensator as Λ_{d1}, which the state space description is omitted for brevity. The quadratic performance levels guaranteed by Theorem 2 for Λ_{s1} and Λ_{d1} are $\gamma = 3.003$ and $\gamma = 2.979$, respectively.

Next, we consider restricting the anti-windup augmentation such that the anti-windup augmentation is suitable for digital prototyping. The LMI region described by $f_{\mathcal{D}3}(s) = \text{diag}(f_{\mathcal{D}1}(s), f_{\mathcal{D}2}(s))$, where $f_{\mathcal{D}2}(s) = ss^* - 350^2$. Applying Theorem 2 and Remark 5 yields the static anti-windup compensator

$$\Lambda_{s,3} = \begin{bmatrix} 0.544 & -0.946 & 0.231 & 0.060 & -0.274 & 0.081 & 36.40 & 19.38 & 0 & 0 \\ 1.153 & -1.267 & 0.507 & -0.020 & 0.031 & -0.101 & -8.517 & 38.61 & 0 & 0 \end{bmatrix}^*$$

and the plant-order dynamic anti-windup compensator, denoted by Λ_{d3}. The quadratic performance levels guaranteed by Theorem 2 for Λ_{s3} and Λ_{d3} are $\gamma = 3.003$ and $\gamma = 2.990$, respectively.

It is evident Λ_{s1} has significantly larger terms than Λ_{s3}, thus inferring larger anti-windup closed loop poles are likely induced. The anti-windup quadratic performance level γ in Table 1 was evaluated via Theorem 1 and $f_{\mathcal{D}1}(s)$. The anti-windup closed loop is a nonlinear dynamic system, thus the magnitudes of the poles are not directly assessed, as in a purely linear system. *Theorem 1* and $f_{\mathcal{D}}(s) = ss^* - \rho^2$ was used to determine a worst case upper bound $\bar{\rho}$ for the magnitudes of the anti-windup closed loop poles as $\gamma \to \infty$. The quantity $\hat{\rho}$ in Table 1 denotes the largest pole for the open (u_m=0) and closed (u_m=u) loop *linear systems* for each case. Note that $\hat{\rho}$ must be less than or equal to $\bar{\rho}$, and both closely agree.

Table 1: Performance and pole magnitude

	(u=u_m)	Λ_{s1}	Λ_{d1}	Λ_{s3}	Λ_{d3}
γ	2.51	3.00	2.98	3.00	2.99
$\bar{\rho}$ [rad/s]	263	3.4×10^3	9.1×10^6	285	271
$\hat{\rho}$ [rad/s]	263	3.4×10^3	9.1×10^6	285	268

The unconstrained case (u_m=u) is the baseline for both the closed loop performance and magnitude of the closed loop poles. The values of $\bar{\rho}$ for both Λ_{s1} and Λ_{d1} are much larger than the Nyquist frequency ω_s≈1571 rad/s. The γ values in Table 1 confirm no discernible performance was lost by restricting the magnitude of the poles. In addition, the plant-order anti-windup compensators did not enable significantly lower values of γ compared to the static anti-windup compensators.

D. Experimental Results

The experiment consists of starting the idle engine at approximately 70 rad/s and the hydraulic motors at rest, and tracking a series of step commands. The *baseline case* (u_m≈u) is limited by only the hardware limitations $\gamma_e\in[0,10]$ volts and $\alpha\in[0,10]$ volts. Note that Λ_{s3} was used to compensate for the brief saturation at startup. The input saturation effects were emphasized by artificially limiting the fuel index and swash plate input to $\gamma_e\in[3.5,7.0]$ volts and $\alpha\in[3.5,6.5]$ volts, respectively.

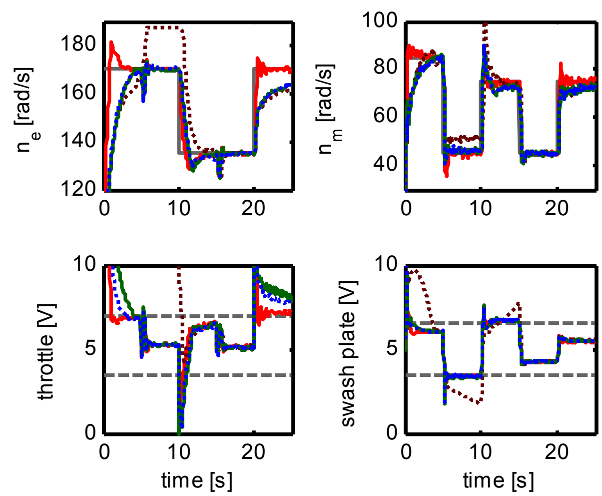

Figure 4: Closed loop response; u_m≈u (solid red), Λ=0 (dotted dark red), Λ_{s3} (solid green), Λ_{d3} (dotted blue)

The fixed-step simulation of the anti-windup compensators Λ_{s1} and Λ_{d1} was observed to be unstable for even the open loop (u_m=0) and closed loop (u_m=u) cases. The Runge-Kutta integration technique is only an approximate integration technique. Specifically, the integration error increases as $\bar{\rho}$ increases for a fixed *sampling time* T_s. Consequently, the unstable simulation was likely caused by the poles that greatly exceeded the Nyquist frequency.

As shown in Figure 4, the *uncompensated case* (Λ=0) exhibited significant performance deterioration due to input saturation. In contrast, the anti-windup compensators greatly improved the performance over the uncompensated case. The anti-windup closed loop systems quickly recovered from input saturations to approximately match the baseline closed loop response.

V. Conclusions

This paper extended the notion of quadratic $\mathcal{D}$-stability to the analysis and design of anti-windup closed loop systems. Theorem 1 established sufficient conditions for the quadratic performance of an anti-windup closed loop system. *Theorem 2* presents sufficient conditions for the existence of an anti-windup compensator that enables a quadratic performance level of γ. Special cases of *Theorem 2* were also briefly discussed in terms of equivalence to several results in the literature. In the practical example, the anti-windup compensator design was applied to an electro-hydraulic testbed. The practical example illustrated how the notion of quadratic $\mathcal{D}$-stability can be a useful tool to restrict the continuous-time anti-windup compensator design for digital prototyping.

References

[1] Boyd, S., El Ghaoui, L., Feron, E. & Balakrishnan, V. *Linear Matrix Inequalities in System and Control Theory*, Society for Industrial and Applied Mathematics , Philadelphia, PA, 1994.

[2] Chilali, M., Gahinet, P. & Apkarian, P. Robust Pole Placement in LMI Regions. *IEEE Transactions on Automatic Control*. 44(12), 2257-2270, 1999.

[3] Gahinet, P., Nemirovski, A., Laub, A. J. & Chilali, M. LMI Control Toolbox. Natick, MA: The MathWorks, Inc, 1995.

[4] Grimm, G., Hatfield, J., Postlethwaite, I., Teel, A.R., Turner, M.C. & Zaccarian, L. "Antiwindup for stable linear systems with input saturation: an LMI-based synthesis," *IEEE Transactions on Automatic Control*. 48(9), 1509-1525, 2003.

[5] Hencey, B. & Alleyne, A. "A static anti-windup compensator design technique for robust regional pole placement," In *Proceedings of the ASME International Mechanical Engineering Congress and Exposition Conference*, Chicago, IL, 2006.

[6] Hencey, B. & Alleyne, A. "A KYP Lemma for LMI Regions," *IEEE Transactions on Automatic Control*, to appear.

[7] Mulder, E. F., Kothare, M. V. & Morari M. "Multivariable anti-windup controller synthesis using linear matrix inequalities," *Automatica*, 37(9), 1407-1416, 2001.

[8] Prempain, E. & Postlethwaite, I. "Extended projection conditions for some structured LMI problems," In *Proceedings of the 38th IEEE Conference on Decision and Control* (pp. 2339-2334), Phoenix, AZ, 1999.

[9] Syaichu-Rohman, A. & Middleton, R. H. "Anti-windup Schemes for discrete-time systems: an LMI-based design. In *Proceedings of the 5th Asian Control Conference*, (pp. 554-561), 2004.

[10] Zhang, R., Alleyne, A. & Prasetiawan, E. "Modeling and $\mathcal{H}_2/\mathcal{H}_\infty$ MIMO control of an earthmoving vehicle powertrain," *ASME Journal of Dynamic Systems, Measurement and Control, Trans. of the ASME*. 124(4), 625-636, 2002.